



AMERICAN METEOROLOGICAL SOCIETY

Bulletin of the American Meteorological Society

EARLY ONLINE RELEASE

This is a preliminary PDF of the author-produced manuscript that has been peer-reviewed and accepted for publication. Since it is being posted so soon after acceptance, it has not yet been copyedited, formatted, or processed by AMS Publications. This preliminary version of the manuscript may be downloaded, distributed, and cited, but please be aware that there will be visual differences and possibly some content differences between this version and the final published version.

The DOI for this manuscript is doi: 10.1175/BAMS-D-15-00245.1

The final published version of this manuscript will replace the preliminary version at the above DOI once it is available.

If you would like to cite this EOR in a separate work, please use the following full citation:

Cordeira, J., F. Ralph, A. Martin, N. Gaggini, R. Spackman, P. Neiman, J. Rutz, and R. Pierce, 2016: Forecasting Atmospheric Rivers during CalWater 2015. Bull. Amer. Meteor. Soc. doi:10.1175/BAMS-D-15-00245.1, in press.

© 2016 American Meteorological Society



Forecasting Atmospheric Rivers During CalWater 2015

Jason M. Cordeira

*Department of Atmospheric Science and Chemistry
Plymouth State University, Plymouth, NH*

F. Martin Ralph and Andrew Martin

*Center for Western Weather and Water Extremes
Scripps Institution of Oceanography
University of California San Diego, La Jolla, CA*

Natalie Gaggini and Ryan Spackman

*Science and Technology Corporation
Boulder, Colorado*

Paul Neiman

*Physical Sciences Division, NOAA/Earth System Research Laboratory
Boulder, Colorado*

Jonathan Rutz

*NOAA/NWS Western Region Headquarters
Salt Lake City, UT*

Roger Pierce

*NOAA/NWS San Diego
San Diego, CA*

Submitted to *BAMS* on 11 March 2016

Revised and Resubmitted to *BAMS* on 31 May 2016

Corresponding Author:

Jason M. Cordeira

Plymouth State University

17 High Street, MSC 48

Plymouth, NH 03264

Phone: (603) 535 2410

Email: j_cordeira@plymouth.edu

39 **Abstract**

40 Atmospheric Rivers (ARs) are long and narrow corridors of enhanced vertically
41 integrated water vapor (IWV) and IWV transport (IVT) within the warm sector of extratropical
42 cyclones that can produce heavy precipitation and flooding in regions of complex terrain,
43 especially along the U.S. West Coast. Several field campaigns have investigated ARs under the
44 “CalWater” program of field studies. The first field phase of CalWater during 2009–2011
45 increased the number of observations of precipitation and aerosols, among other parameters,
46 across California and sampled ARs in the coastal and near-coastal environment, whereas the
47 second field phase of CalWater during 2014–2015 observed the structure and intensity of ARs
48 and aerosols in the coastal and offshore environment over the Northeast Pacific. This manuscript
49 highlights the forecasts that were prepared for the CalWater field campaign in 2015 and the
50 development and use of an “AR portal” that was used to inform these forecasts. The AR portal
51 contains archived and real-time deterministic and probabilistic gridded forecast tools related to
52 ARs that emphasize water vapor concentrations and water vapor flux distributions over the
53 eastern North Pacific, among other parameters, in a variety of formats derived from the NCEP
54 Global Forecast System and Global Ensemble Forecast System. The tools created for the
55 CalWater 2015 field campaign provided valuable guidance for flight planning and field activity
56 purposes, and may prove useful in forecasting ARs and better anticipating hydrometeorological
57 extremes along the U.S. West Coast.

58 **Introduction**

59 *a. What is an atmospheric river?*

60 Atmospheric Rivers (ARs) are broadly defined as long and narrow corridors of strong
61 water vapor transport that are characterized by enhanced vertically integrated water vapor (IWV)
62 and enhanced IWV transport (IVT) (e.g., Ralph et al. 2004; Neiman et al. 2008). The IWV and
63 IVT corridors associated with ARs are typically >2000 km long and 500–1000 km wide and
64 often represent areas of instantaneous poleward and lateral moisture transport in the warm-sector
65 of midlatitude cyclones (e.g., Ralph et al. 2006; Dacre et al. 2015). These corridors often extend
66 from the subtropics into the extratropics and contribute substantially to the occurrence of
67 orographic precipitation events over the western U.S. (Ralph and Dettinger 2012). AR-related
68 precipitation events constitute a large portion (~30–50%) of annual precipitation and play a
69 primary role in water resources management and water supply across the western U.S. (e.g.,
70 Dettinger et al. 2011). In fact, California’s annual precipitation varies far more than most of the
71 country, and 85% of the variance in annual precipitation in northern California results from
72 annual variations in the top 5% wettest days per year, which are mostly attributed to water vapor
73 flux along landfalling ARs (Dettinger and Cayan 2014). The purpose of this paper is to highlight
74 different tools that were developed and used to analyze and forecast the location, intensity,
75 duration, and potential landfall of regions of water vapor transport along ARs during an
76 observing campaign over the Northeast Pacific during January–March 2015 named CalWater
77 2015.

78

79 *b. What is CalWater?*

80 CalWater is a multi-year program of field campaigns, numerical modeling efforts and
81 scientific analyses focused on phenomena that are key to water supply and associated extremes
82 (e.g., drought, flood) across the western U.S. (Ralph et al. 2015). The first field phase of
83 CalWater during 2009–2011, i.e., “CalWater 1”, (1) increased the number of observations of
84 precipitation and aerosols, among other parameters, in the Sierra Nevada, Central Valley, and
85 coastal region in California via the installation of the western-region National Oceanic and
86 Atmospheric Administration (NOAA) Hydrometeorological Testbed (HMT-West; Ralph et al.
87 2013a) and (2) sampled ARs in the coastal and near-coastal environment with the Department of
88 Energy (DOE) G-1 aircraft. The second field phase of CalWater, i.e., “CalWater 2”, is a multi-
89 year effort that included field campaign during February 2014, during January–March 2015, and
90 includes anticipated field campaigns during 2016–2018. CalWater 2 collectively focuses on
91 observations of the structure and intensity of ARs in the coastal and offshore environment over
92 the eastern North Pacific. The CalWater 2 field campaign during January–March 2015, hereafter
93 referred to as CalWater 2015, employed four research aircraft: the NOAA G-IV and P-3
94 aircrafts, the DOE G-1 aircraft, and the National Aeronautics and Space Administration (NASA)
95 ER-2 aircraft, as well as the NOAA research vessel (RV) Ron Brown, which carried other DOE
96 sensors. The National Science Foundation and DOE also sponsored an overlapping major aerosol
97 and cloud measurement experiment at the coast called the Atmospheric Radiation Measurement
98 (ARM) Cloud Aerosol Precipitation Experiment (ACAPEX) during January–March 2015.
99 Additional information on the scientific objectives of the CalWater field campaigns can be found
100 in Ralph et al. (2015). Additional information on ACAPEX can be found online at
101 <http://www.arm.gov/campaigns/amf2015apex> and additional information on the DOE ARM
102 facilities used in ACAPEX is found in Schmid et al. (2014).

103

104 *c. Motivation and Objective*

105 Planning efforts by the CalWater 2015 “Forecasting Working Group” (Ralph et al. 2015)
106 identified the specific forecast needs for field operations and led to the formation of a “forecast
107 team” that provided timely forecasts of the location, intensity, duration, and possible landfall of
108 ARs in the offshore and near-coastal environment in support of field activities. The team was
109 comprised of three early-career scientists that acted as lead forecasters and additional forecasters
110 from several academic institutions, two NOAA National Weather Service (NWS) Weather
111 Forecast Offices, the NOAA/NWS Western Region Headquarters, the NOAA Earth Systems
112 Research Laboratory (ESRL) and the Science and Technology Corporation (Table 1). A
113 complementary team of forecasters also comprised the “aerosol forecast team” for ACAPEX.
114 The AR forecasts were used for short-term (~1–3 days) flight and ship planning activities and
115 long-term (~1–2 weeks) strategic planning for observing ARs with a single platform or multiple
116 coincident platforms. The remainder of this paper highlights different tools that were developed
117 to better forecast the location, intensity, duration and possible landfall of ARs, and their
118 implementation during CalWater 2015.

119

120 **The AR Portal**

121 An “AR portal” was developed for various applications and was first tested significantly
122 during CalWater 2015 in order to analyze and forecast the intensity, duration, and landfall of
123 ARs during the experiment. The AR portal contains archived and real-time observations, gridded
124 analyses, and gridded numerical weather prediction (NWP) forecasts of AR-related information
125 over the Northeast Pacific and western U.S. (<http://arportal.ucsd.edu>). The observations on the

126 AR portal during CalWater 2015 included: (1) Geostationary Operational Environmental
127 Satellite (GOES) imagery provided by NOAA; (2) Special Sensor Microwave Imager (SSM/I)-
128 derived total precipitable water imagery provided by the Cooperative Institute for Meteorological
129 Satellite Studies (CIMSS); (3) gridded analyses and point observations of precipitation provided
130 by the California–Nevada River Forecast Center, the National Weather Service Advanced
131 Hydrologic Prediction Service, and the Community Collaborative Rain, Hail & Snow Network;
132 and (4) multi-instrument observations from the Coastal Atmospheric River Monitoring and Early
133 Warning System at Bodega Bay, Chico, and Colfax in California provided by the NOAA ESRL.
134 The gridded analyses and forecasts on the AR portal during CalWater 2015 were created from
135 NCEP Global Forecast System (GFS) and Global Ensemble Forecast System (GEFS) data
136 provided by the NOAA Operational Model Archive and Distribution System (NOMADS). All
137 data manipulations and images were generated using the National Center for Atmospheric
138 Research (NCAR) Command Language (NCAR 2016) and were hosted at the Center for
139 Western Weather and Water Extremes at the Scripps Institution of Oceanography and at
140 Plymouth State University. These gridded analyses and NWP forecasts complemented existing
141 tools that were used by forecasters to identify analyzed and forecasted locations of ARs based on
142 IWV provided by the NOAA ESRL Physical Science Division AR Detection Tool (ARDT; Wick
143 et al. 2013). A list of the AR-related GFS and GEFS gridded products that were created and
144 supported CalWater 2015 is provided in Table 2.

145 The AR-related gridded forecast products focus on identifying and tracking ARs over the
146 Northeast Pacific with attention to their structure, intensity, and orientation at landfall along the
147 U.S. West Coast. The gridded forecast products feature plan-view, cross-section, and time-series
148 analyses and forecasts of the IWV, horizontal water vapor flux, and the IVT vector, among other

149 parameters. A large number of the gridded analysis and forecast products illustrate the IVT
150 vector, which has been used to study ARs since 2008 (Neiman et al. 2008). Note that a majority
151 (75%) of IVT within ARs is confined to the lower 2.25 km of the troposphere where heavy
152 orographic precipitation may result in regions of water vapor flux that intersect mountainous
153 terrain along the U.S. West Coast (Ralph et al. 2005). Cross section analyses and forecasts were
154 particularly helpful in identifying the vertical distribution of water vapor flux relative to coastal
155 terrain during periods with landfalling ARs. Further motivation for incorporating the IVT vector
156 into the forecast process is provided by a pair of studies by Lavers et al. (2014, 2016) that
157 demonstrate the IVT distribution is potentially more predictable with ~1–2 days of advanced
158 lead time over the North Atlantic and North Pacific Oceans than the corresponding NWP-derived
159 quantitative precipitation forecast (QPF). These results suggest that NWP-derived forecasts of
160 the IVT vector might provide enhanced situational awareness for ARs over the North Pacific and
161 North Atlantic prior to landfall along the U.S. and European West Coasts.

162 Common thresholds used for identifying ARs from gridded analysis and forecast data
163 over the Northeast Pacific include a combination of IWV values ≥ 20 mm and IVT magnitudes
164 $\geq 250 \text{ kg m}^{-1} \text{ s}^{-1}$ as discussed in Rutz et al. (2014). The IVT distribution, however, is often used
165 in order to better emphasize the transport of water vapor and its role in precipitation instead of
166 just the presence of water vapor illustrated by the IWV distribution. The daily average IVT
167 magnitude (IWV) explains ~50% (~25%) of the variance in 24-h precipitation across the western
168 U.S. (Rutz et al. 2014). The IVT magnitude $\geq 250 \text{ kg m}^{-1} \text{ s}^{-1}$ threshold is therefore chosen in part
169 because ARs with IVT magnitudes $\geq 250 \text{ kg m}^{-1} \text{ s}^{-1}$ have a larger impact on precipitation
170 distributions across the western U.S. than coinciding areas of IWV values ≥ 20 mm according to
171 Rutz et al. (2014). These thresholds may not apply universally across all ocean basins, but have

172 shown viability in identifying the locations of ARs over the Northeast Pacific and locations of
173 landfalling ARs along the U.S. West Coast. Similar thresholds for water vapor flux have also
174 been developed for observational data that cannot explicitly calculate IVT magnitude. For
175 example, Neiman et al. (2009) and Ralph et al. (2013b) calculate the bulk upslope water vapor
176 flux as the product of terrain-normal lower-tropospheric profiler-derived winds and IWV, and
177 define “AR conditions” at coastal locations (i.e., landfall) in northern California as $IWV \geq 20$ mm
178 and bulk upslope water vapor flux ≥ 150 mm m s⁻¹. The bulk upslope water vapor flux explains
179 up to 75% of the variance in total precipitation that results from forced saturated ascent during
180 landfalling ARs at coastal locations in northern California (Ralph et al. 2013b).

181 Displays of IVT and other gridded forecast parameters were computed from the
182 deterministic GFS and 20-member GEFS data. The GEFS IVT forecasts were displayed as
183 thumbnail and probability-over-threshold maps over the Northeast Pacific, multi-member time-
184 series diagrams (e.g., a plume or dispersion diagram) for locations along the U.S. West Coast,
185 and as a probability-over-threshold in a time-latitude framework for locations along the U.S.
186 West Coast. The probability-over-threshold analysis is computed as the fraction of GEFS
187 ensemble members with IVT magnitudes ≥ 250 kg m⁻¹ s⁻¹, and the time-latitude analysis follows
188 latitude and longitude locations along the U.S. West Coast in lieu of locations along a meridian.

189

190 **CalWater 2015 Implementation**

191 *a. Forecast Process*

192 The CalWater 2015 field campaign spanned from 12 January to 8 March 2015. The
193 forecast team provided a weather briefing each morning from the field campaign operations
194 center at McClellan Airfield outside Sacramento, CA to mission scientists at 0800 PST (i.e.,

195 1600 UTC); each weather briefing was preceded by a coordination call with the NWS at 0700
196 PST. The weather briefings focused on (1) the location and intensity of ARs that were platform
197 targets over the Northeast Pacific, and the timing and duration of AR conditions along the U.S.
198 West Coast in both short-term (e.g., 1–3 days) and medium-term (e.g., 3–7 days) forecasts, (2)
199 probable locations and intensity of ARs over the Northeast Pacific and along the U.S. West
200 Coast in long-term forecasts (e.g., 7–10+ days), and (3) local weather conditions for aircraft
201 activities at the time of take off and landing. The weather briefings concluded with aerosol- and
202 precipitation-related forecasts for the ACAPEX campaign and platform (flight, coastal
203 observatories, and ship) planning activities. The weather briefings were followed by a detailed
204 written summary of the weather briefing, and “now-casting” support for flight activities that
205 typically ended between 1600 and 2000 PST (i.e., 0000 and 0400 UTC). These weather briefings
206 and written summaries are also archived and available on the AR portal.

207

208 *b. Case Study Illustration of Forecast and Analysis Tools*

209 An example of a timeline and continuity graphic provided to mission scientists during the
210 weather briefing at 5 February 2015 schematically illustrates the approximate location of AR
211 corridors (i.e., forecaster-identified axes of $IVT \geq 250 \text{ kg m}^{-1} \text{ s}^{-1}$ from gridded forecast data) over
212 the Northeast Pacific during 5–8 February 2015 (Fig. 1a). The collocation of an AR corridor with
213 the location of the NOAA RV Ron Brown facilitated a coordinated, multi-platform intensive
214 operational period (IOP) over the Northeast Pacific later on 5 February 2015 that also included
215 in-situ observations by the NOAA G-IV and P-3, NASA ER-2, and DOE G-1 aircrafts. This AR,
216 and a subsequent AR, was further observed by campaign observing systems and the suite of
217 instrumentation located across the HMT-West network (Fig. 1b) during landfall along the U.S.

218 West Coast during 6–8 February 2015. A coastal atmospheric river observatory (ARO; White et
219 al. 2009) site located at Bodega Bay (BBY), CA documented the landfall of these two ARs in
220 association with two periods of enhanced IWV ≥ 20 mm (values exceeded 30 mm), strong lower-
221 tropospheric southwesterly flow, enhanced bulk upslope water vapor flux values ≥ 150 mm m s⁻¹
222 (values exceeded 800 mm m s⁻¹), and hourly precipitation amounts > 8 mm h⁻¹ on 6–7 February
223 2015 and on 8 February 2015 (Fig. 2)

224 The shorter-term (~84-h) gridded GFS forecasts of the 6–7 February 2015 ARs were used
225 for flight planning purposes several days in advance. The deterministic 84-h gridded GFS
226 forecast initialized at 1200 UTC 3 February 2015 illustrated the nose of a strong (> 750 kg m⁻¹
227 s⁻¹) corridor of southwest-to-northeast oriented IVT along an AR over coastal regions of central
228 California at 0000 UTC 7 February 2015 (Fig. 3a). The location and timing of this AR in the 84-
229 h forecast verified within a very small margin of error (< 100 km and < 3 h) with respect to the 0-
230 h analysis at 0000 UTC 7 February 2015, whereas the intensity of IVT along the AR was under
231 forecast by > 250 kg m⁻¹ s⁻¹ (Fig. 3b; note the planned NOAA G-IV flight track based on the
232 forecasted IVT distribution). Figure 3c provides an accompanying analysis of Global Positioning
233 System-derived IWV observations across the western U.S. that are available on the AR Portal
234 that are also able to assist in verifying IWV-based definitions of AR conditions (e.g., IWV values
235 ≥ 20 mm). The position error of this particular AR at landfall in the 84-h forecast is well below
236 the average root-mean square position error of ~500 km for global NWP models identified by
237 Wick et al. (2013). Many locations along the U.S. West Coast, as well as California’s Sierra
238 Nevada and Washington’s Cascades, ultimately received > 100 mm of precipitation during the
239 120-h period ending at 1200 UTC 9 February 2015; several locations received > 400 mm of
240 precipitation (not shown).

241 The longer-term gridded GEFS forecasts issued 1–2 weeks prior to the 5–8 February
242 2015 ARs were used to plan the coordinated, multi-platform IOPs that took place offshore on 5
243 February 2015 and onshore during 6–8 February 2015 (Figs. 4 and 5). For example, the
244 ensemble 168-h GEFS IVT thumbnail forecasts initialized at 0000 UTC 31 January 2015
245 illustrate overall agreement in the orientation (e.g., southwest-to-northeast) of IVT along an AR
246 but considerable variability in the maximum intensity of IVT along an AR over the Northeast
247 Pacific (e.g., maximum IVT magnitudes range between $750 \text{ kg m}^{-1} \text{ s}^{-1}$ and $>1500 \text{ kg m}^{-1} \text{ s}^{-1}$)
248 and timing of landfall (i.e., $\text{IVT} \geq 250 \text{ kg m}^{-1} \text{ s}^{-1}$ at coastal locations) at 0000 UTC 7 February
249 2015 (Fig. 4). Time series forecasts of 0-to-16-day ensemble-member IVT magnitude initialized
250 at 0000 UTC 28 January 2015 (Fig. 5a) and at 0000 UTC 31 January 2015 (Fig. 5b) illustrate
251 similar variability in the intensity and timing, and also duration of AR conditions ($\text{IVT} \geq 250 \text{ kg}$
252 $\text{m}^{-1} \text{ s}^{-1}$) at 38°N , 123°W along the U.S. West Coast. The 0000 UTC 28 January 2015 GEFS
253 forecast illustrated ensemble-member average IVT magnitudes $\geq 250 \text{ kg m}^{-1} \text{ s}^{-1}$ between \sim 0000
254 UTC 7 February 2015 and \sim 0000 UTC 8 February 2015 (\sim 24 h; Fig. 5a), whereas the 0000 UTC
255 31 January 2015 GEFS forecast illustrated ensemble-member average IVT magnitudes $\geq 250 \text{ kg}$
256 $\text{m}^{-1} \text{ s}^{-1}$ between \sim 0000 UTC 6 February 2015 and \sim 0000 UTC 9 February 2015 (\sim 72 h; Fig. 5b).
257 The GEFS thumbnail and time series forecasts suggested considerable uncertainty in the timing,
258 duration, and intensity of AR conditions at coastal locations during 6–8 February 2015. This
259 uncertainty is also illustrated via the corresponding 0-to-16-d GEFS time-latitude probability-
260 over-threshold forecasts along the U.S. West Coast initialized at 0000 UTC on 28 January 2015
261 (Fig. 5c) and 0000 UTC 31 January 2015 (Fig. 5d). This “AR landfall tool” highlighted
262 probabilities of AR conditions ($\text{IVT} \geq 250 \text{ kg m}^{-1} \text{ s}^{-1}$) $>50\%$ as early as \sim 10 days in advance for
263 many locations along the U.S. West Coast, and when initializations were viewed in sequence

264 every six hours, provided valuable information on run-to-run consistency and increasing
265 likelihoods of AR conditions beginning in north-coastal California and Oregon and proceeding
266 south along the California coast over time.

267

268 **Summary**

269 ARs are long and narrow corridors of enhanced IVT and IWV within the warm sector of
270 extratropical cyclones that can produce heavy precipitation and flooding in regions of complex
271 terrain, especially along the U.S. West Coast. ARs have been and continue to be the foci of
272 several multi-year field campaigns under the CalWater umbrella (Ralph et al. 2015) that aim to
273 better observe ARs over the eastern North Pacific, in the near-coastal, and onshore environments.
274 Forecasts of ARs for the CalWater 2015 field campaign made by a team of early-career scientists
275 and participants from academic institutions and government agencies were informed by an AR
276 portal that was created in order to provide a clearinghouse for observations, gridded analysis and
277 gridded forecast tools related to ARs over the Northeast Pacific and over the western U.S. The
278 gridded analysis and forecast tools created for the CalWater 2015 field campaign provided
279 valuable guidance for flight planning and other field activity purposes. These analyses and
280 forecast tools, or adapted versions thereof, may also be useful in the day-to-day analysis and
281 forecasts of ARs along the U.S. West Coast by weather forecasters and water managers to better
282 anticipate hydrometeorological extremes. These adapted analyses and forecast tools may serve
283 as a part of a decision support system that could provide AR-related forecasts for high-profile
284 locations near reservoirs to aid in predicting water supply or forecast-informed reservoir
285 operations (Ralph et al. 2014), vulnerable infrastructure as described by the 2009 Howard
286 Hanson Dam flood risk management crisis (White et al. 2012), watersheds to aid in streamflow

287 prediction, floods, and flash floods (Neiman et al. 2011), or recent wildfire burn scars to aid in
288 diagnosing debris flow or landslide susceptibility (White et al. 2013).

289

290 *Acknowledgments*

291 The creation of the AR portal and participation for the lead author in CalWater 2015 was
292 supported by NOAA grant #NA13OAR4830231 and the State of California-Department of
293 Water Resources award #4600010378, both as part of broader projects led by the University of
294 California San Diego, Scripps Institution of Oceanography's Center for Western Weather and
295 Water Extremes. Student participation from Plymouth State University in CalWater 2015 was
296 supported by NASA Space Grant #NNX10AL97H. The authors are grateful for comments
297 provided by Benjamin Moore (University at Albany) and two anonymous reviewers that greatly
298 improved the quality of this manuscript.

299

300 **For Further Reading**

301 Dacre, H. F., P. A. Clark, O. Martinez-Alvarado, M. A. Stringer, and D. A. Lavers, 2015: How
302 do atmospheric rivers form? *Bull. Amer. Meteor. Soc.*, 96, 1243–1255, doi:10.1175/
303 BAMS-D-14-00031.1.

304 Dettinger, M. D., F. M. Ralph, T. Das, P. J. Neiman, and D. Cayan, 2011: Atmospheric Rivers,
305 floods, and the water resources of California. *Water*, **3**, 455–478.

306 Dettinger, M. D., and D. Cayan, 2014: Drought and the California Delta—A matter of extremes:
307 San Francisco Estuary and Watershed Science, 12(2), 7 p,
308 <http://escholarship.org/uc/item/88f1j5ht>.

309 Lavers, D. A., F. Pappenberger, and E. Zsoter 2014: Extending medium-range predictability of

310 extreme hydrological events in Europe. *Nature Communications*, **5**, 1–7.

311 Lavers, D. A., D. E. Waliser, F. M. Ralph and M. D. Dettinger, 2016: Predictability of horizontal
312 water vapor transport relative to precipitation: Enhancing situational awareness for
313 forecasting western U.S. extreme precipitation and flooding. *Geophysical Research
314 Letters*, **43**, doi:10.1002/2016GL067765.

315 NCAR, 2016: The NCAR Command Language (Version 6.3.0) [Software]. (2016). Boulder,
316 Colorado: UCAR/NCAR/CISL/TDD. <http://dx.doi.org/10.5065/D6WD3XH5>

317 Neiman, P. J., F. M. Ralph, G. A. Wick, J. D. Lundquist, and M. D. Dettinger, 2008:
318 Meteorological characteristics and overland precipitation impacts of atmospheric rivers
319 affecting the West Coast of North America based on eight years of SSM/I satellite
320 observations. *J. Hydrometeor.*, **9**, 22–47.

321 Neiman P. J., A. B. White, F. M. Ralph, D. J. Gottas and S. I. Gutman, 2009: A water vapor flux
322 tool for precipitation forecasting. *Water Manage.*, **162** (2), 83–94.

323 Neiman, P. J., L. J. Schick, F. M. Ralph, M. Hughes, and G. A. Wick, 2011: Flooding in western
324 Washington: The connection to atmospheric rivers. *J. Hydrometeor.* **12**, 1337–1358.

325 Ralph, F. M., and M. D. Dettinger, 2012: Historical and national perspectives on extreme west
326 coast precipitation associated with atmospheric rivers during December 2010. *Bull. Amer.
327 Meteor. Soc.*, **93**, 783–790.

328 Ralph, F. M., P.J. Neiman, and G.A. Wick, 2004: Satellite and CALJET aircraft observations of
329 atmospheric rivers over the Eastern North Pacific Ocean during the winter of 1997/98.
330 *Mon. Wea. Rev.*, **132**, 1721–1745.

331 Ralph, F. M., P. J. Neiman, and R. Rotunno, 2005: Dropsonde observations in low-level jets over
332 the Northeastern Pacific Ocean from CALJET-1998 and PACJET-2001: mean vertical-
333 profile and atmospheric-river characteristics. *Mon. Wea. Rev.*, **133**, 889–910.

334 Ralph, F. M., P. J. Neiman, G. Wick, S. Gutman, M. Dettinger, D. Cayan, and A. B. White,
335 2006: Flooding on California’s Russian River—role of atmospheric rivers. *Geophys. Res.*
336 *Lett.*, **33**, (L13801), 5 pp.

337 Ralph, F.M., and coauthors, 2013a: The emergence of weather-focused testbeds linking research
338 and forecasting operations. *Bull. Amer. Meteor. Soc.*, **94**, 1187–1210.

339 Ralph, F. M., T. Coleman, P.J. Neiman, R. Zamora, and M.D. Dettinger, 2013b: Observed
340 impacts of duration and seasonality of atmospheric-river landfalls on soil moisture and
341 runoff in coastal northern California. *J. Hydrometeor.*, **14**, 443–459.

342 Ralph, F. M., and coauthors, 2014: A vision for future observations for Western U.S. extreme
343 precipitation and flooding— Special Issue of *J. Contemporary Water Resources Research*
344 *and Education*, Universities Council for Water Resources, Issue 153, 16–32.

345 Ralph, F. M., and coauthors, 2015: CalWater. *Bull. Amer. Meteor. Soc.*, *in press*.

346 Rutz, J. J., W. J. Steenburgh, and F. M. Ralph, 2014: Climatological characteristics of
347 atmospheric rivers and their inland penetration over the Western United States. *Mon.*
348 *Wea. Rev.*, **142**, 905–921.

349 Schmid, B., and coauthors, 2014: The DOE ARM aerial facility. *Bull. Amer. Met. Soc.*, **95**, 723–
350 742.

351 White, A. B., F. M. Ralph, P. J. Neiman, D. J. Gottas, and S. I. Gutman, 2009: The NOAA
352 coastal atmospheric river observatory. Preprints, *34th Conf. on Radar Meteorology*,

353 Williamsburg, VA, Amer. Meteor. Soc., 10B.4. [Available online at
354 <http://ams.confex.com/ams/pdfpapers/155601.pdf>.]

355 White, A. B., and coauthors, 2012: NOAA's Rapid Response to the Howard A. Hanson Dam
356 Flood Risk Management Crisis. *Bull. Amer. Meteorol. Soc.*, **93**, 189–207, doi:
357 10.1175/BAMS-D-11-00103.1.

358 White, A.B., and coauthors, 2013: A 21st century California observing network for monitoring
359 extreme weather events. *J. Atmos. Ocean. Technol.*, **30**, 1585–1603.

360 Wick, G. A., P. J. Neiman, F. M. Ralph, and T. M. Hamill, 2013: Evaluation of forecasts of the
361 water vapor signature of atmospheric rivers in operational numerical weather prediction
362 models. *Wea. Forecasting*, **28**, 1337–1352, doi:10.1175/WAF-D-13-00025.1.

363
364

365 **List of Tables**

366
367 TABLE 1. List of individuals who participated on the AR forecast team, affiliation, and their role
368 in CalWater 2015.

Individual	Affiliation	Role
Jason Cordeira	Plymouth State University	Forecast team lead and Lead forecaster
Natalie Gaggini	Science and Technology Corporation	Lead forecaster
Jonathan Rutz	NOAA/NWS Western Region HQ	Lead forecaster and NWS coordinator
Roger Pierce	NOAA/NWS San Diego	NWS coordinator
William Rasch	NOAA/NWS Sacramento	NWS coordinator
Paul Neiman	NOAA/ESRL	Forecaster
Brian Kawzenuk	Plymouth State University	Forecaster
Klint Skelly	Plymouth State University	Forecaster
Vanessa Almanza	University of Hawaii at Manoa	Forecaster
Michael Mueller	CIRES, University of Colorado	Forecaster

369

370 TABLE 2. List of archived and real-time gridded analyses and gridded forecasts from the GFS
 371 and that were available on the AR portal during CalWater 2015.

Model	Analysis type	Analysis and Forecast Fields	Frequency and Location
GFS	Map	Integrated water vapor (IWV) Eulerian IWV tendency and budget Vertically integrated water vapor transport (IVT) Time-integrated IVT Sea-level pressure Precipitation rate 900-hPa wind vector 900-hPa potential temperature 900-hPa equivalent potential temperature 900-hPa geopotential height 850-hPa wind vector 500-hPa geopotential height 500-hPa wind vector 500-hPa absolute vorticity 300-hPa wind vector and Isotachs	Every 3 h from 0 to 72 h Every 6 h from 72 to 168 h Every 12 h from 168 h to 240 h Over two domains: domain 1 spanned 16–66°N and 160–110°W, whereas domain 2 spanned 25–50°N and 140–115°W ¹
GFS	Map	Total precipitation	5- and 7-d totals over domain 1
GFS	Cross section, time series	Water vapor flux Freezing level IWV and IVT magnitude	Every 6 h from 0 to 60 h Along 135°W, 130°W, 125°W, and 120°W for 25°–50°N
GFS	Time-height, time series	Water vapor flux Relative humidity Wind vector Freezing level 3-h precipitation IWV and IVT magnitude	Every 3 h from 0 to 72 h Every 3 h from 0 to 168 h Locations every 1° latitude × 1° longitude over a domain spanning 30°–50°N and 115°–135°W
GEFS	Thumbnail maps	IVT magnitude and direction	Every 24 h from 0 h to 384 h Over domain 1
GEFS	Probability maps	Fraction of ensemble with IVT magnitude $\geq 250 \text{ kg m}^{-1} \text{ s}^{-1}$	Every 24 h from 0 h to 384 h Over domain 1
GEFS	Time-latitude	Fraction of ensemble with IVT magnitude $\geq 250 \text{ kg m}^{-1} \text{ s}^{-1}$ or $\geq 500 \text{ kg m}^{-1} \text{ s}^{-1}$	Every 6 h from 0 h to 384 h For locations along coast
GEFS	Time series	Ensemble member IVT magnitude	Every 6 h from 0 h to 384 h For locations along coast

¹ The domain was adjusted westward later in the field campaign in order to accommodate temporary flight activities based out of Hawaii.

372

373 **List of Figures**

374 Fig. 1. (a) An example of the time continuity of AR corridors at 1600 PST (i.e., 0000 UTC;
375 shown as bold lines, with the corresponding dates shown in M/D format where M = month and D
376 = day) used during CalWater 2015 for flight planning and field activities. The example was used
377 in the forecast process on Thursday, 5 February 2015. The location of the NOAA RV Ron
378 Brown (yellow star) and the approximate 2.5-hour flight range of the NOAA G-IV aircraft (red
379 semicircle) are indicated. The sequence of green, black, and dashed gray arrows correspond to
380 one propagating AR, the sequence of solid gray and smaller blue lines correspond to a second
381 AR, and the longer solid blue and purple lines correspond to a third AR. (b) An annotated
382 analysis of the HMT-West observing network as shown in Fig. 2b of White et al. (2013), with
383 the location of the Bodega Bay (BBY), CA “atmospheric river observatory” highlighted by the
384 yellow arrow and latitude and longitude locations that follow the U.S. West Coast in California
385 used in Fig. 4 denoted by the “×” symbols.

386

387 Fig. 2. Time series analysis of meteorological conditions at Bodega Bay (BBY), CA for 6–8
388 February 2015. Top panel: Time-height analysis of horizontal wind from a 449 MHz profiler
389 color shaded according to magnitude (m s^{-1}); middle panel: surface wind speed (m s^{-1} ; blue line)
390 and direction (dashed black line); bottom panel: bulk upslope WV Flux (mm m^{-1} ; red dashed
391 line, calculated according to the methodology of Neiman et al. 2009), hourly precipitation (mm;
392 blue line), and IWV (mm; black dashed contour).

393

394 Fig. 3. (a) 84-h NCEP GFS gridded forecast of IVT magnitude ($\text{kg m}^{-1} \text{s}^{-1}$; shaded according to
395 scale) and direction (vectors plotted according to scale and for magnitudes $\geq 250 \text{ kg m}^{-1} \text{s}^{-1}$)

396 initialized at 1200 UTC on 3 February 2015; (b) as in (a), except for the verifying analysis of
397 IVT magnitude and direction at 0000 UTC 7 February 2015 with overlaid draft flight track of the
398 NOAA G-IV aircraft (the track follows the numbers in sequence as drawn where point 4 would
399 correspond most closely in time to the aircraft location at 0000 UTC); (c) GPS-derived IWV
400 (mm; shaded according to scale) at 0015 UTC 7 February 2015.

401

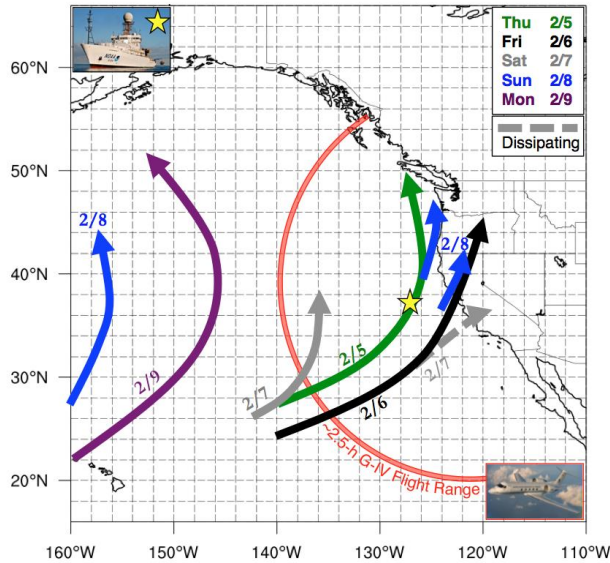
402 Fig. 4. 168-h NCEP GEFS gridded forecasts of IVT (plotted as in Figs. 3a,b) initialized at 0000
403 UTC 31 January 2015 for each of the 20 ensemble members valid at 0000 UTC 7 February 2015.

404

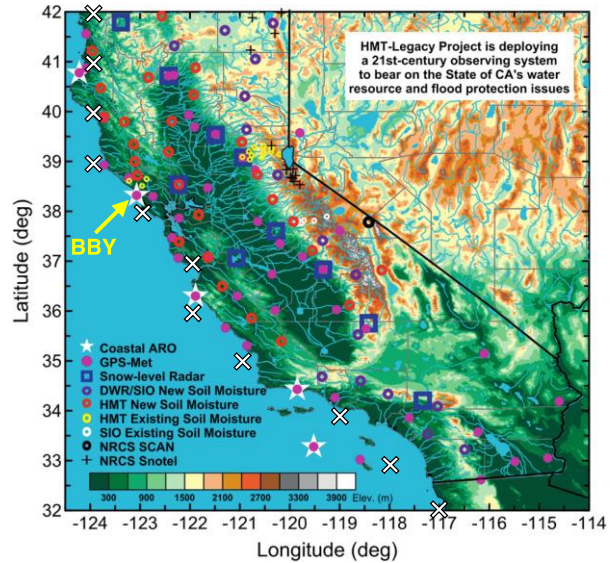
405 Fig. 5. Time series diagrams of the 16-d forecast of IVT magnitude ($\text{kg m}^{-1} \text{s}^{-1}$) at 38°N , 123°W
406 initialized at (a) 0000 UTC 28 January 2015 and (b) 0000 UTC 31 January 2015 for each NCEP
407 GEFS ensemble member (thin black lines), the control member (solid black line), and the
408 ensemble mean (green line). The red and blue lines represent the maximum and minimum IVT
409 magnitudes at each forecast hour, whereas the white shaded regions represent the spread about
410 the mean (± 1 standard deviation) of the ensemble at each forecast hour. A 16-day forecast time-
411 “latitude” (where latitude follows the U.S. West Coast) depiction of the fraction of GEFS
412 ensemble members (including the control member) with IVT magnitudes $\geq 250 \text{ kg m}^{-1} \text{ s}^{-1}$
413 (shaded according to scale; left panels) initialized at (a) 0000 UTC 28 January 2015 and (b) 0000
414 UTC 31 January 2015. The vertical dashed black lines denote the time of 0000 UTC 7 February
415 2015 in panels a–d, whereas the dashed horizontal line denotes 38°N in panels c–d. The latitude
416 and longitude locations that follow the U.S. West Coast for California between 32°N and 42°N
417 are shown in Fig. 1b.

418 **Figures**

a. AR Continuity Forecast

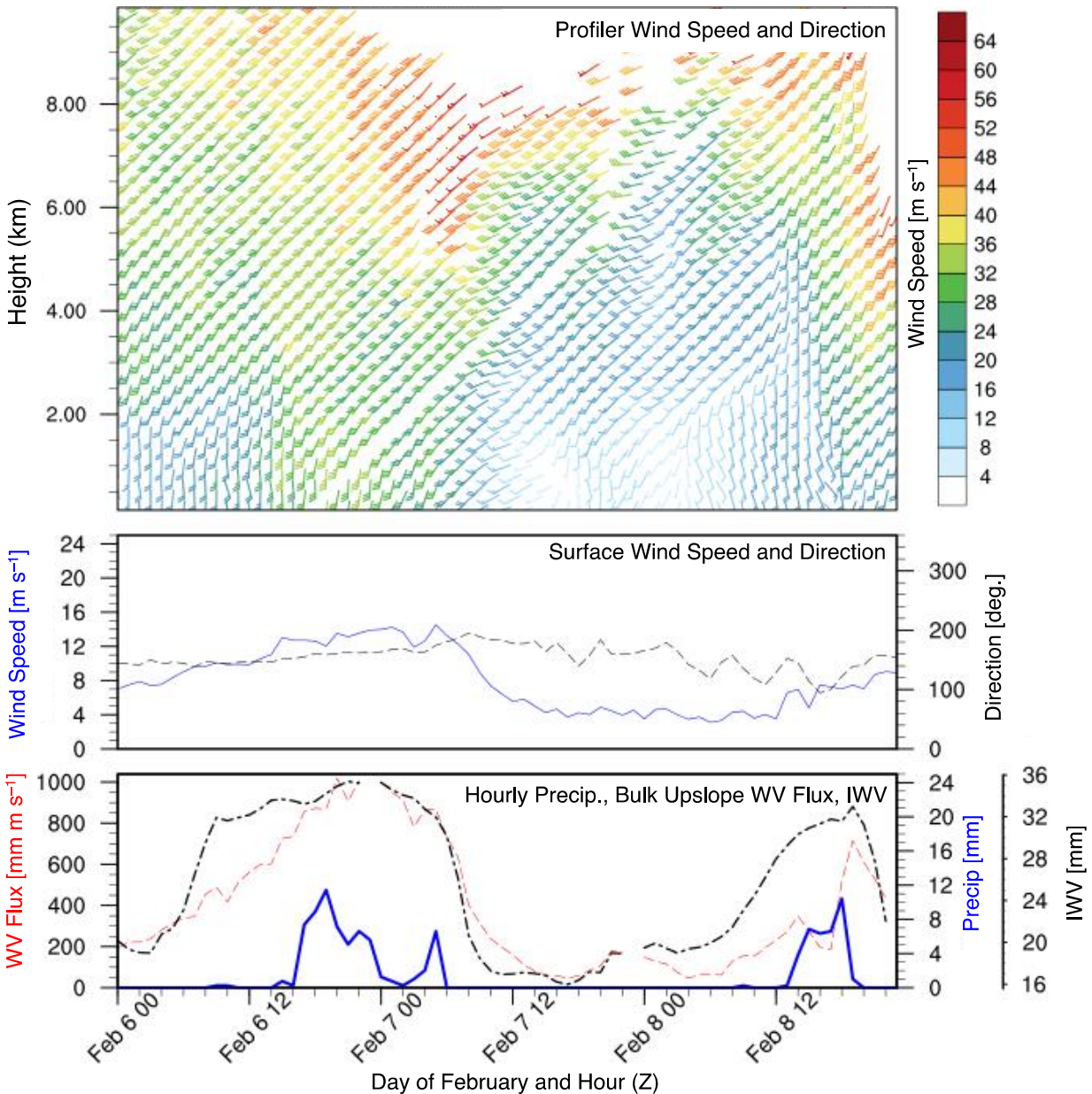


b. Locations of HMT Network Observations



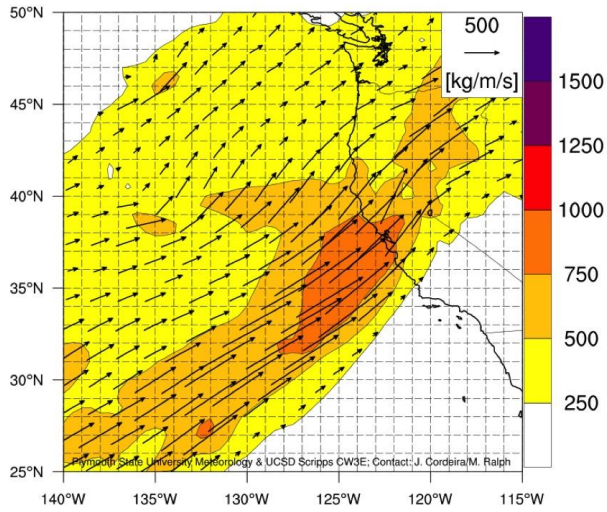
419
 420 Fig. 1. (a) An example of the time continuity of AR corridors at 1600 PST (i.e., 0000 UTC;
 421 shown as bold lines, with the corresponding dates shown in M/D format where M = month and D
 422 = day) used during CalWater 2015 for flight planning and field activities. The example was used
 423 in the forecast process on Thursday, 5 February 2015. The location of the NOAA RV Ron
 424 Brown (yellow star) and the approximate 2.5-hour flight range of the NOAA G-IV aircraft (red
 425 semicircle) are indicated. The sequence of green, black, and dashed gray arrows correspond to
 426 one propagating AR, the sequence of solid gray and smaller blue lines correspond to a second
 427 AR, and the longer solid blue and purple lines correspond to a third AR. (b) An annotated
 428 analysis of the HMT-West observing network as shown in Fig. 2b of White et al. (2013), with
 429 the location of the Bodega Bay (BBY), CA “atmospheric river observatory” highlighted by the
 430 yellow arrow and latitude and longitude locations that follow the U.S. West Coast in California
 431 used in Fig. 4 denoted by the “x” symbols.
 432

Time series data for Bodega Bay, CA, 6–8 Feb 2015

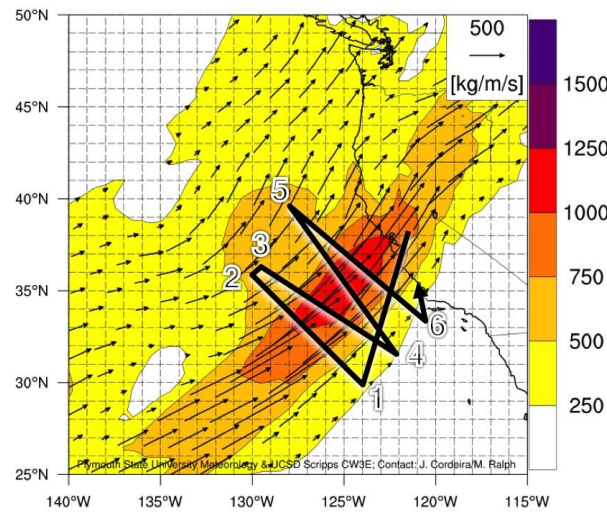


433
 434 Fig. 2. Time series analysis of meteorological conditions at Bodega Bay (BBY), CA for 6–8
 435 February 2015. Top panel: Time-height analysis of horizontal wind from a 449 MHz profiler
 436 color shaded according to magnitude (m s^{-1}); middle panel: surface wind speed (m s^{-1} ; blue line)
 437 and direction (dashed black line); bottom panel: bulk upslope WV Flux (mm m s^{-1} ; red dashed
 438 line, calculated according to the methodology of Neiman et al. 2009), hourly precipitation (mm;
 439 blue line), and IWV (mm; black dashed contour).
 440

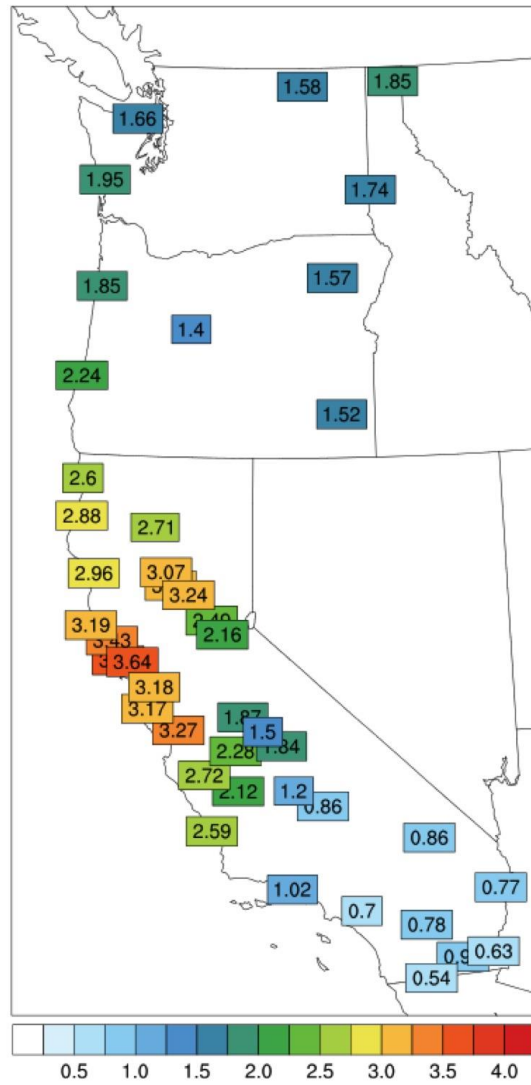
a. 84-h IVT forecast valid 00Z 7 Feb 2015



b. 0-h IVT analysis valid 00Z 7 Feb 2015

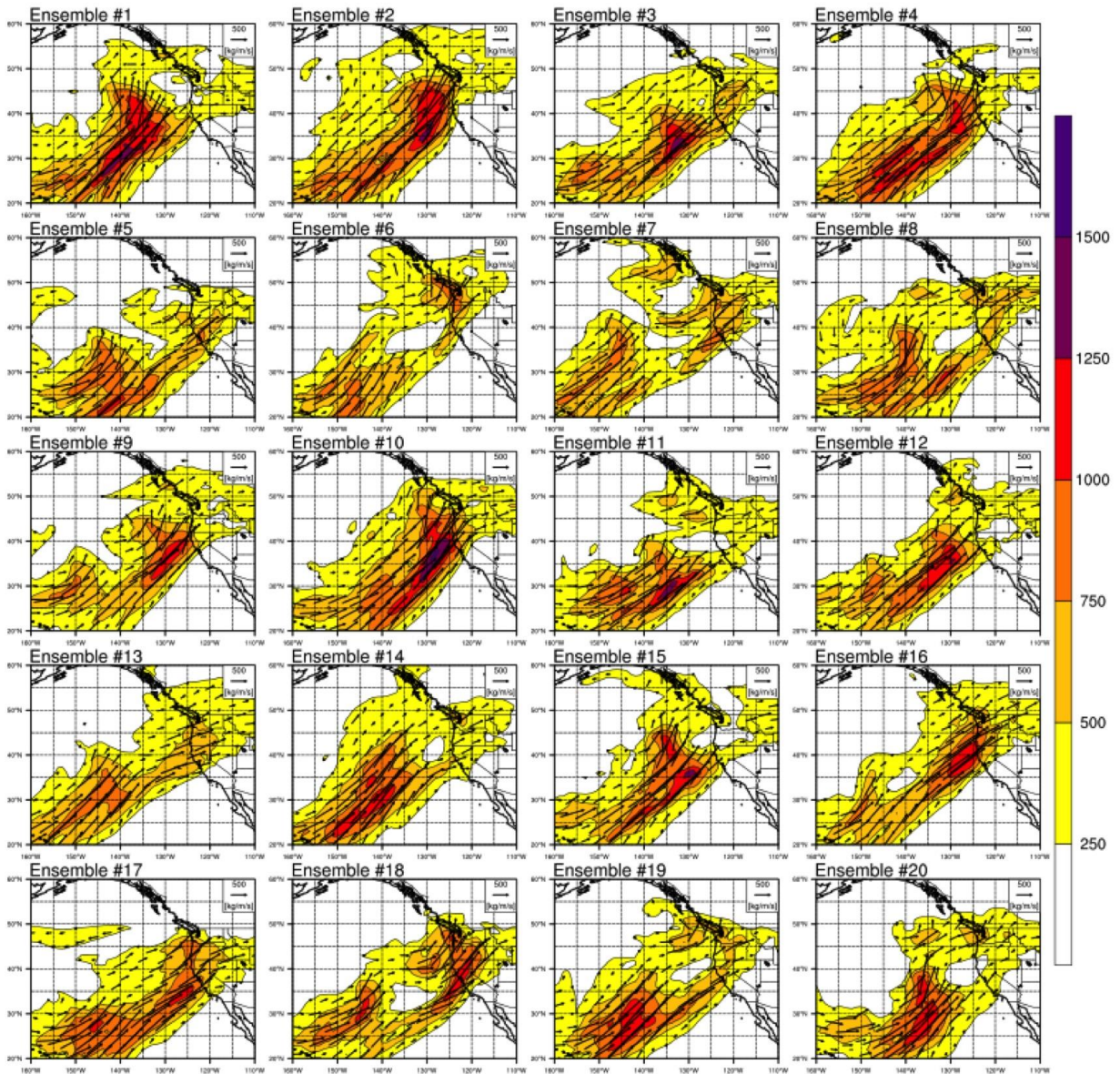


c. GPS IWV, 0015 UTC 7 Feb 2015



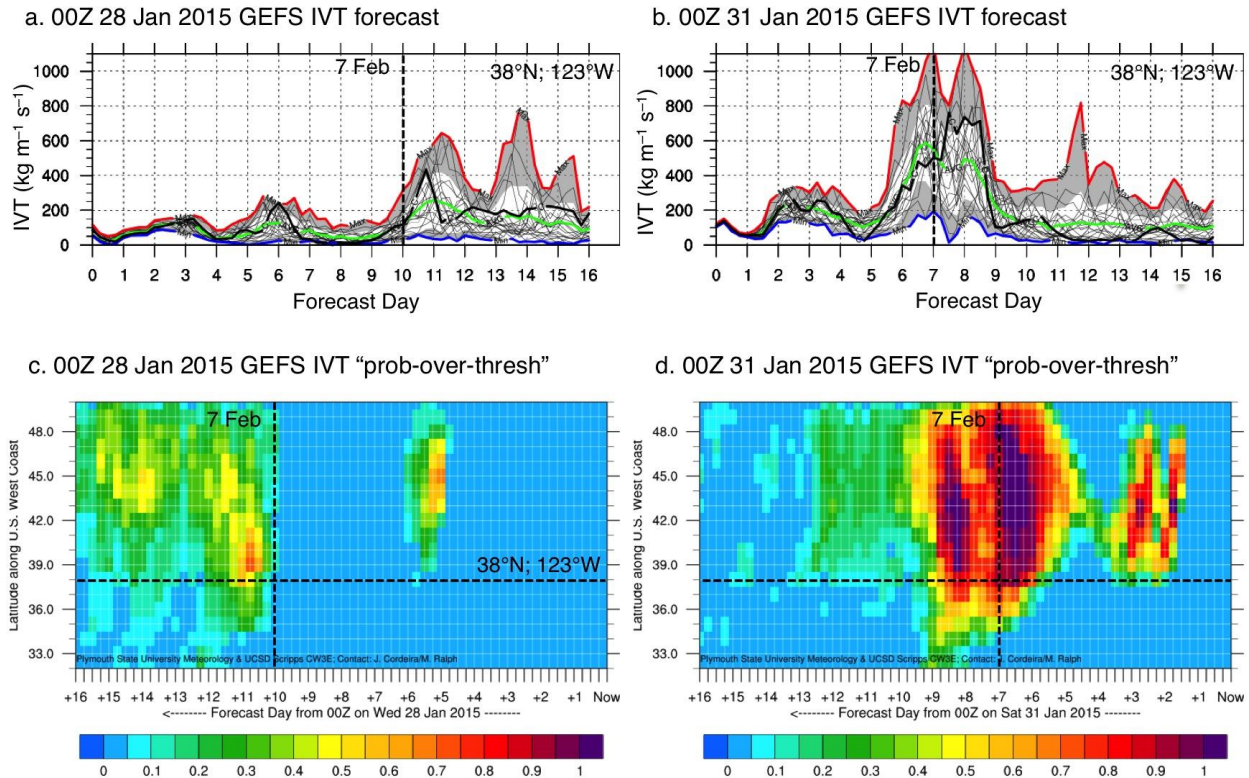
441
 442 Fig. 3. (a) 84-h NCEP GFS gridded forecast of IVT magnitude ($\text{kg m}^{-1} \text{s}^{-1}$; shaded according to
 443 scale) and direction (vectors plotted according to scale and for magnitudes $\geq 250 \text{ kg m}^{-1} \text{s}^{-1}$)
 444 initialized at 1200 UTC on 3 February 2015; (b) as in (a), except for the verifying analysis of
 445 IVT magnitude and direction at 0000 UTC 7 February 2015 with overlaid draft flight track of the
 446 NOAA G-IV aircraft (the track follows the numbers in sequence as drawn where point 4 would
 447 correspond most closely in time to the aircraft location at 0000 UTC); (c) GPS-derived IWV
 448 (mm; shaded according to scale) at 0015 UTC 7 February 2015.
 449

168-h GEFS IVT ($\text{kg m}^{-1} \text{s}^{-1}$) forecast initialized at 0000 UTC 31 Jan 2015, valid 0000 UTC 7 Feb 2015



450
451
452

Fig. 4. 168-h NCEP GEFS gridded forecasts of IVT (plotted as in Figs. 3a,b) initialized at 0000 UTC 31 January 2015 for each of the 20 ensemble members valid at 0000 UTC 7 February 2015.



453
 454 Fig. 5. Time series diagrams of the 16-d forecast of IVT magnitude ($\text{kg m}^{-1} \text{s}^{-1}$) at 38°N , 123°W
 455 initialized at (a) 0000 UTC 28 January 2015 and (b) 0000 UTC 31 January 2015 for each NCEP
 456 GEFS ensemble member (thin black lines), the control member (solid black line), and the
 457 ensemble mean (green line). The red and blue lines represent the maximum and minimum IVT
 458 magnitudes at each forecast hour, whereas the white shaded regions represent the spread about
 459 the mean (± 1 standard deviation) of the ensemble at each forecast hour. A 16-day forecast time-
 460 “latitude” (where latitude follows the U.S. West Coast) depiction of the fraction of GEFS
 461 ensemble members (including the control member) with IVT magnitudes $\geq 250 \text{ kg m}^{-1} \text{ s}^{-1}$
 462 (shaded according to scale; left panels) initialized at (a) 0000 UTC 28 January 2015 and (b) 0000
 463 UTC 31 January 2015. The vertical dashed black lines denote the time of 0000 UTC 7 February
 464 2015 in panels a–d, whereas the dashed horizontal line denotes 38°N in panels c–d. The latitude
 465 and longitude locations that follow the U.S. West Coast for California between 32°N and 42°N
 466 are shown in Fig. 1b.